

Research Article

TiO₂-Based Organic Hybrid Solar Cells with Mn⁺² Doping

Zühal Alparslan,¹ Arif Kösemen,^{1,2} Osman Örnek,^{1,3} Yusuf Yerli,¹ and S. Eren San¹

¹Organic Electronics Research Group, Department of Physics, Gebze Institute of Technology, 41400 Gebze, Turkey

²Department of Physics, Muş Alparslan University, 49100 Muş, Turkey

³Department of Physics, Sakarya University, 54187 Sakarya, Turkey

Correspondence should be addressed to Yusuf Yerli, yusufyerli@gmail.com

Received 22 February 2011; Revised 9 April 2011; Accepted 24 April 2011

Academic Editor: Mohamed Sabry Abdel-Mottaleb

Copyright © 2011 Zühal Alparslan et al. This is an open access article distributed under the Creative Commons Attribution License, which permits unrestricted use, distribution, and reproduction in any medium, provided the original work is properly cited.

A hybrid solar cell is designed and proposed as a feasible and reasonable alternative, according to acquired efficiency with the employment of TiO₂ (titanium dioxide) and Mn-doped TiO₂ thin films. In the scope of this work, TiO₂ (titanium dioxide) and Mn:TiO₂ hybrid organic thin films are proposed as charge transporter layer in polymer solar cells. Poly(3-hexylthiophene):phenyl-C61-butyric acid methyl ester (P3HT:PCBM) is used as active layer. When the Mn-doped TiO₂ solar cells were compared with pure TiO₂ cells, Mn-doped samples revealed a noteworthy efficiency enhancement with respect to undoped-TiO₂-based cells. The highest conversion efficiency was obtained to be 2.44% at the ratio of 3.5% (wt/wt) Mn doping.

1. Introduction

Main criteria in choosing material for photovoltaic devices are feasibility and environmental convenience, as well as compatibility to solar spectra and easy and cheap production [1]. Organic-based materials are promising for photovoltaic applications [2–4] with advantageous features such as low cost, easy production, and flexible application. Therefore, organic solar cells are serious candidates in place of silicon solar cells [5]. Although organic-based materials are satisfying with most of these mentioned criteria, charge transport properties of these materials are not so good and their efficiency is still quite low. To overcome this problem, in recent studies, bulk heterojunction structure of the n-type PCBM and p-type P3HT materials was used [6–9] and 4–5% efficiencies were obtained [10]. The PEDOT:PSS used as an anode buffer layer in this kind of cells is acidic and hygroscopic. Also, ITO is quite susceptible against the acidic corruptions [11]. Therefore, PEDOT:PSS-based solar cells are known to be unstable in air conditions and under light illumination [12–14]. Moreover, in these devices, electron collecting a metal cathode (e.g., Al, Ca) with low work function must be used but they are easily oxidized and lead to deterioration in performance. In order to get rid of these

problems, inverted solar cells have been used with inorganic materials [15–18]. In inverted organic solar cells, the anode is an air-stable high-work-function metal collecting holes such as Ag. The ITO is also used as the cathode to collect electrons. Previous works reveal that conventional solar cells could merely endure for 4 days while inverted solar cells still preserve almost 80% of their efficiency even 40 days later [19]. However, power conversion efficiencies of inverted solar cells are less than those of the conventional organic solar cells. One of the reasons is the bad quality of interface in these inverted designs. These worse interface conditions deteriorate exciton formation and separation [20]. There are various studies to cope with mentioned interface problems [21].

When the polymer active layer in organic solar cell is exposed to the light, excitons begin to form. Excitons diffuse to donor-acceptor interface. In here, they dissociate to form bound electron-hole pair. To separate this pairs into free holes and electrons, there should be an electric field. With the effect of the electric field produced by the work function difference of both electrodes, these free charges are transported to positive and negative electrodes. Since the polymer has a disordered structure, there exists charge carrier loss during transportation through polymer skeleton.

Inorganic materials are used with organics so that ordered continuous paths are provided to charge transfer. This kind of designs are called hybrid systems, and for this aim, various inorganic materials are used in solar cells such as ZnO [22], CdTe [23], PbS [24], and so forth. TiO_2 [20, 25, 26] is also an attractive alternative among these materials. Usage of TiO_2 electrode in dye-based solar cell by Gratzel et al. could be given as a successful application of this material [27]. There are various works to understand the structural changes occurred when TiO_2 is doped by metal ions. In particular, photocatalytic and magnetic properties were investigated by [28, 29]. In the result of such investigations, it was understood that photoreactivity, charge carrier recombination rates, and interfacial electron transfer rates were changed by metal ion doping [30]. Doped TiO_2 is widely used in solar cell applications, and there are several comparative works. In one of them, it has been reported that power conversion efficiency was achieved to be 8% with the dye-based solar cells prepared by nitrogen-doped TiO_2 while 6% efficiency with pure TiO_2 [31]. Also, K. H. Ko et al. performed another work in which TiO_2 was doped with Al and W elements for dye-based solar cells. In Al-doped cells, while open-circuit voltage (V_{OC}) has increased, short-circuit current (I_{SC}) has decreased. As for W-doped cells, a behavior opposite to Al-doped cells was observed [32].

In this work, hybrid solar cells were produced and characterized with ITO/ TiO_2 /P3HT:PCBM/Ag configuration. The novelty and goal of this work comes from the employment of Mn^{+2} ions for the first time with this configuration, in which different amounts of Mn were incorporated to TiO_2 and cell parameters were investigated in terms of doping amount. It was explicitly observed that solar cell efficiency was being improved with Mn doping until a certain doping amount, which is 3.5%. One of the inspirations of choosing Mn^{+2} ion in our aim comes from some works such as [33], which reveals the fact that although the Mn^{+2} ion is slightly larger than Ti^{+4} , the general crystal structure is not changed with doping but light interaction of modified TiO_2 .

2. Experimental

P3HT (Aldrich) and PCBM (Aldrich) were used in the structure of active layer without any further purification. Their chemical formulas are given in Figure 1. P3HT and PCBM were firstly mixed in chlorobenzene with 1:0.8 (wt/wt) ratio at 60°C for a night. In order to prepare TiO_2 sol-gel mixture, titanium n-butoxide, ethanol, isopropanol alcohol, and acetic acid were mixed with (1:20:20:0.15) molar ratio, respectively, for two days at room temperature. Also, MnCl_2 was added into a solution containing a mixture of ethanol, isopropanol alcohol, and acetic acid. This solution of mixture was stirred for two hours at room temperature, and then titanium n-butoxide was added to this sol-gel mixture so that Mn-doped TiO_2 sample was prepared. Ti amount in the solution of mixture is proportional to the amount of Mn, at ratio of their weights. The Mn amounts in samples were prepared as 0.5%, 1.5%, 3.5%, 8.5%, 15%, and 25%.

In regard to the solar cell fabrication process, ITO-coated glass was firstly subject to a standard cleaning process

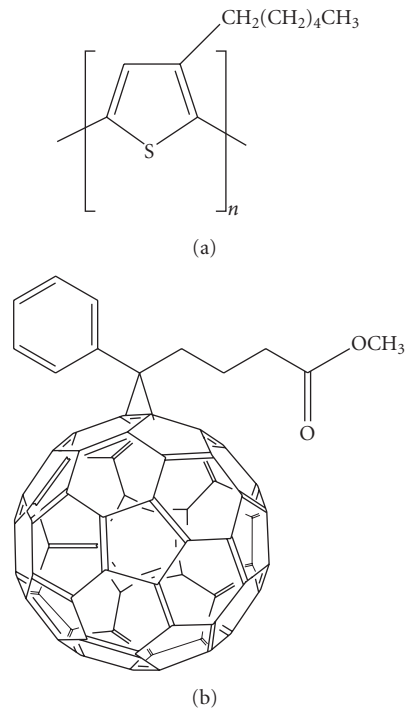


FIGURE 1: Chemical formulas of (a) P3HT and (b) PCBM.

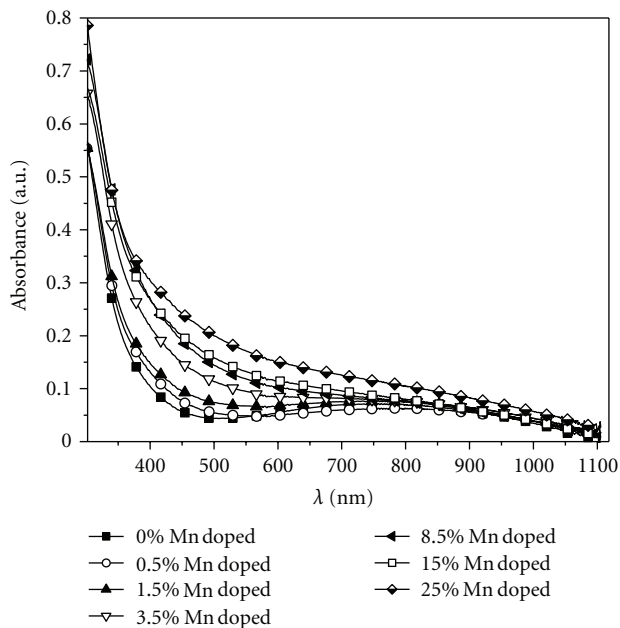


FIGURE 2: Absorption spectra of pure, 0.5%, 1.5%, 3.5%, 8.5%, 15%, and 25% doped TiO_2 films.

with acetone, ethanol, and distilled water in ultrasonic bath for 15 minutes to each cleaning agent. Later, TiO_2 - and Mn-doped TiO_2 gels were coated with spin coater at 3500 rpm. These thin films were annealed at 400°C for 30 min, which was reached in steps of $10^\circ\text{C}/\text{min}$. The solar cells were designed with ITO/ TiO_2 /P3HT:PCBM/Ag and ITO/ TiO_2 :Mn/P3HT:PCBM/Ag configuration. TiO_2

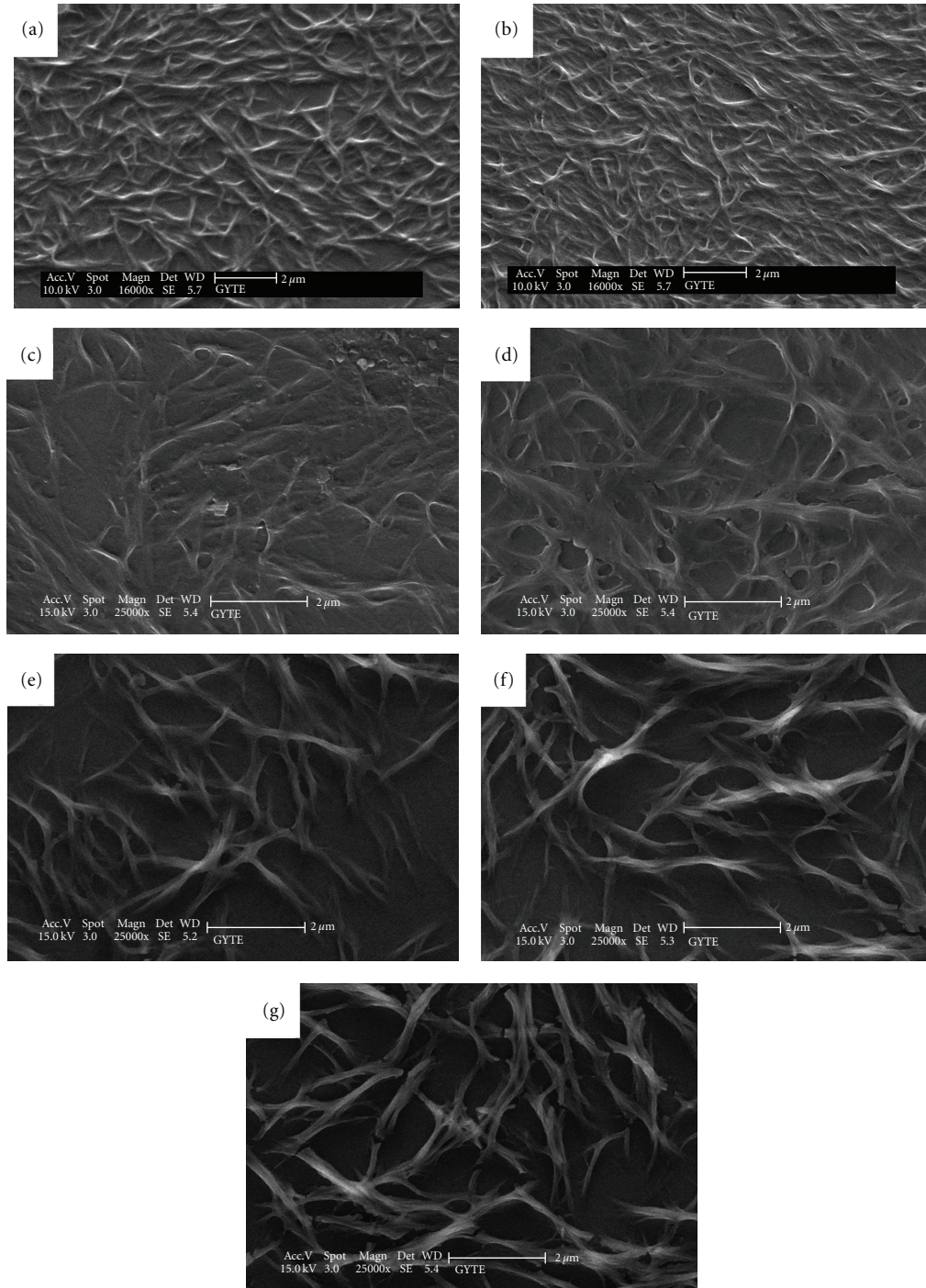


FIGURE 3: SEM pictures of pure (a), 0.5% (b), 1.5% (c), 3.5% (d), 8.5% (e), 15% (f), and 25% (g) doped TiO₂ films.

and doped TiO₂ films were coated with the mixture of P3HT:PCBM as active layer at 2500 rpm. After this, Ag contact layers were deposited at approximately thickness of 100 nm with thermal evaporator. Current-voltage characteristics of the samples were analyzed with (Keithley 4200 SCS) semiconductor characterization system and (Thermo Oriol) Solar Simulator under AM1.5 G (100 mW/cm²) standard characterization regulations. Solar Simulator was calibrated with reference photodiode.

3. Result and Discussion

Figure 2 depicts the UV-Vis absorbance spectra of TiO₂- and Mn-doped TiO₂ films. As the doping percentage of Mn increases, the absorbance curves shift to visible region. In fact, it is supposed that this shift is caused by the diffusion of Mn atoms into TiO₂ lattice. The shift implies that the energy levels of Mn atoms placed in TiO₂ lattice are between the band gap of TiO₂ and the contribution to the light-induced

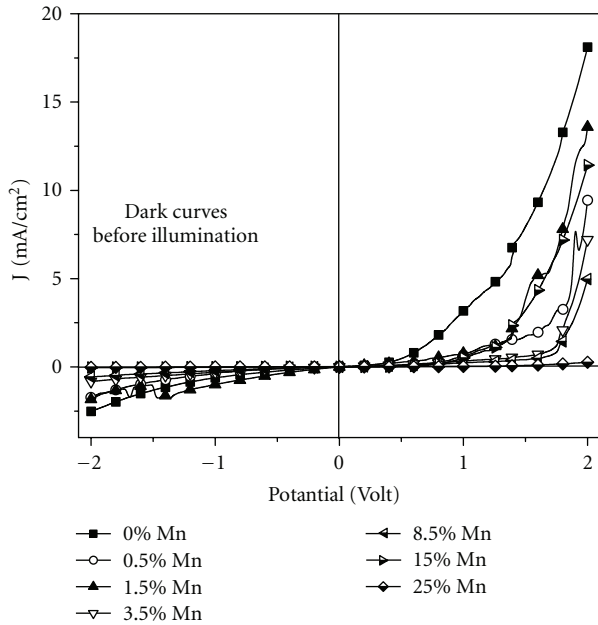


FIGURE 4: J-V characteristic curves for TiO_2 - and Mn-doped TiO_2 solar cells under dark circumstances (before any illumination process).

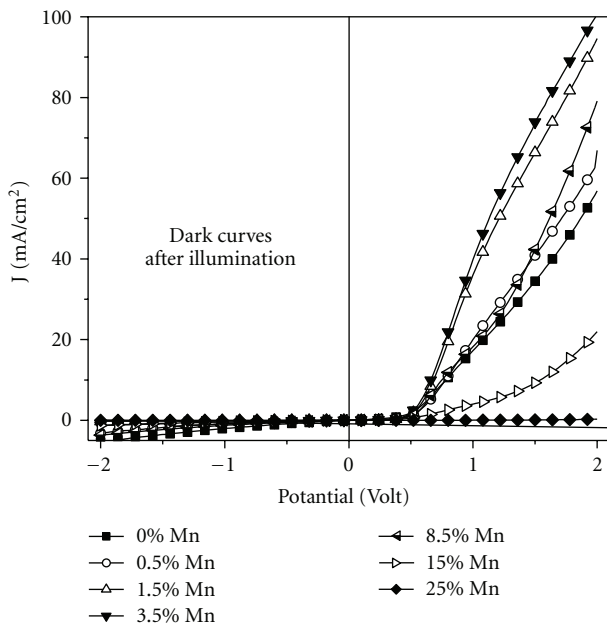


FIGURE 5: J-V characteristic curves for TiO_2 - and Mn-doped TiO_2 solar cells under dark circumstances (after 60-minute illumination).

charge transfer [34]. Also, these kinds of red shifts are related to the charge transfer between d-electrons of metal ions and valance or conduction band of TiO_2 [35]. The SEM pictures of TiO_2 - and Mn-doped TiO_2 films are given in Figure 3. The SEM pictures show the growing of weak skeletons in the case of Pure TiO_2 as shown in Figure 3(a). As the Mn doping percentage is further increased, branches of the skeleton are getting stronger and these stronger branches are yielding an

obvious fiber structures particularly as seen in Figures 3(f) and 3(g).

Figure 4 shows the dark J-V characteristic curves of solar cells prepared by Mn-doped and pure TiO_2 films. The forward bias current of pure- TiO_2 -based cells is bigger than that of the Mn-based cells. That is, injection current is more in pure TiO_2 cells. This indicates the presence of an injection barrier imposed by Mn doping. The same cells are subject to the same measurements under dark conditions again, but this time these cells are exposed to illumination for 60 minutes before dark J-V measurements (Figure 5). This time, the obtained results are entirely different from previous measurements. Forward bias current has increased in all cells, but this increase is much more in 0.5%, 1.5%, 3.5%, and 8.5% doping percentages. In the case of 15% and 25% Mn-doped TiO_2 cells, the increasing tendency of the forward bias current is disrupted. This indicates that there is a threshold value of the Mn doping in our solar cell design. When the cells are exposed to illumination, both photoexcitation and thermal-excitation play an important role in increasing the number of charge carriers in (P3HT : PCBM) active layer and highly photoreactive TiO_2 layers. This could be recognized to be the cause of the increase in current. Also, the injection barrier mentioned for the Mn-doped cells is eliminated when the cells are waited under illumination, so forward bias currents are becoming more with respect to the pure TiO_2 based cells.

The highest forward bias current and maximum power conversion efficiency were observed in 3.5% Mn-doped solar cell. The J-V plots of pure TiO_2 and Mn-doped TiO_2 -based solar cells under illuminated conditions are shown in Figure 6. The power conversion efficiency parameters obtained from these graphs are given in Table 1. There is no improvement in the pure TiO_2 solar cell when the cell is subject to a light illumination even if forward bias current slightly changes due to the heating of the cell. Whereas, even very little amount of Mn doping, for example 0.5%, causes an S-shape in reverse bias in the J-V curves, as soon as illumination starts. In this study as the solar cells were exposed to continuous illumination, the S-shape disappears. After two minutes, it converted conventional solar cell shape for % 0.5 Mn doped. This was observed in all Mn-doped TiO_2 cells. In a work, this kind of S-shape curves was previously explained with electrical dipoles occurred at the interface [36]. In another study, it is expressed that the reason for S-shaped curve is charge accumulation near one of the electrodes [37]. As for our cells, the reason for S-shaped curve (Figure 6) was the accumulation of the charge occurring in TiO_2 due to Mn doping.

ITO/ TiO_2 /P3HT:PCBM/Ag solar cells are actually the inverted structures, and light is absorbed in P3HT active layer. The excitons, which are produced in polymer active layer, are separated at P3HT/PCBM interface, and free electrons are diffused to ITO side by passing through TiO_2 while the free holes are diffused to Ag side as represented in Figure 7. It is obvious that the reason of S-shaped curve is the Mn(II) ions, since there is no such a shape in pure- TiO_2 -containing cells, as seen in Figure 6. In regard to possible mechanism of this event, one can think that either the

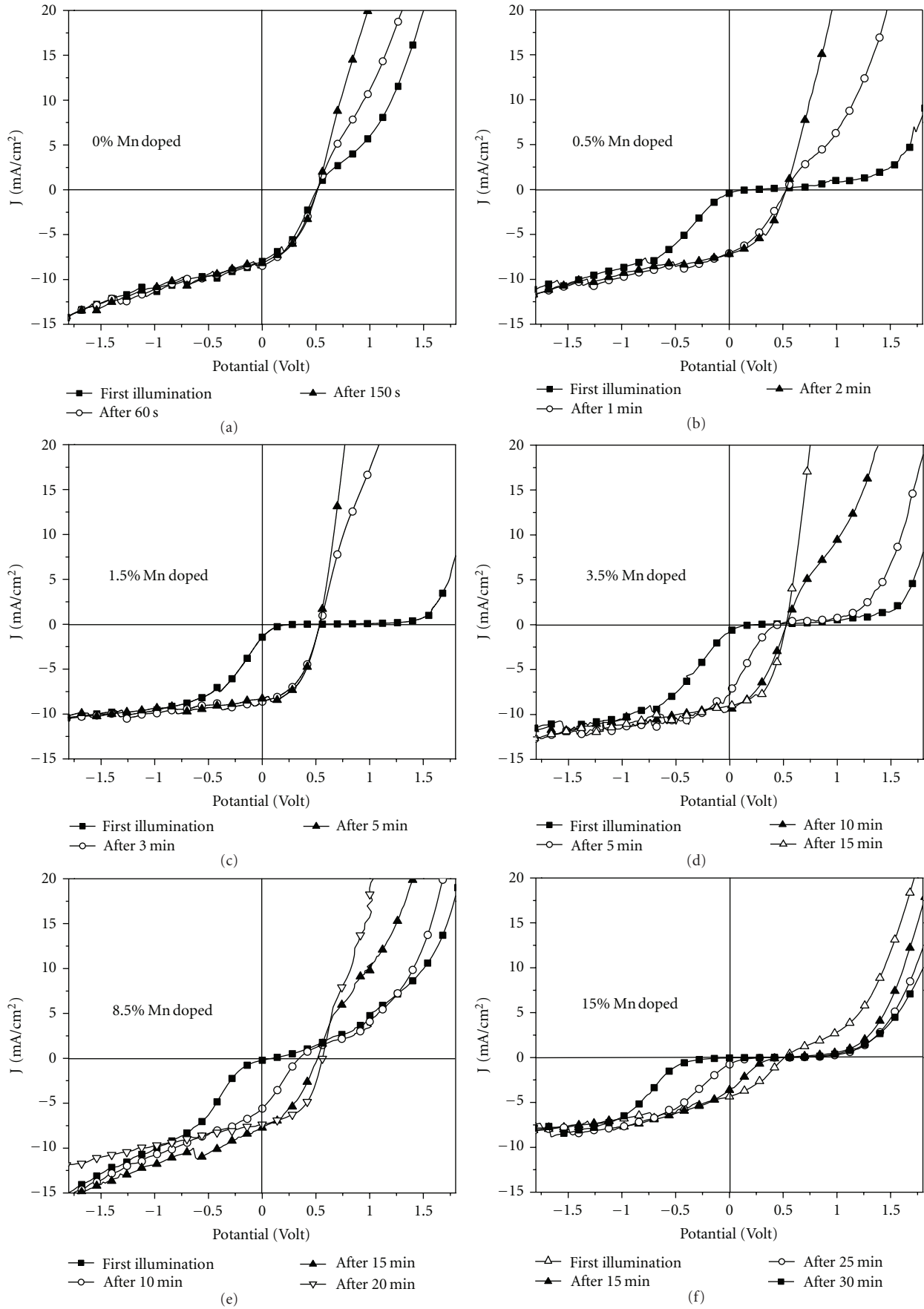


FIGURE 6: Continued.

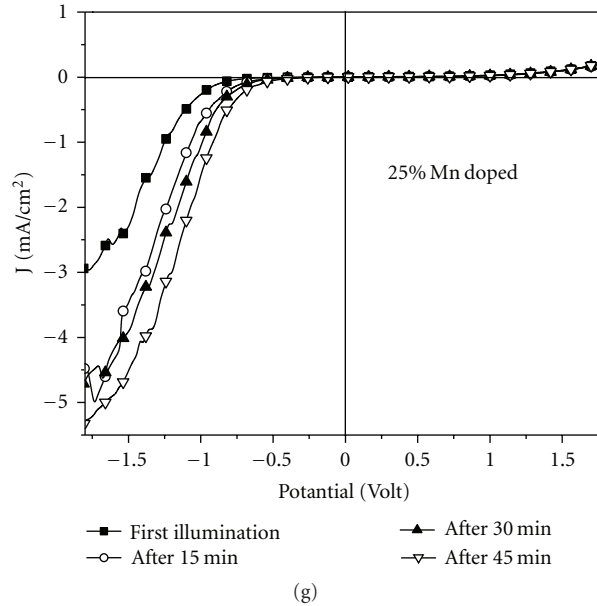


FIGURE 6: J-V characteristic curves for TiO₂- and Mn-doped TiO₂ solar cells under illumination.

TABLE 1: Designed solar cells power conversion parameters.

Mn doped	FF (%)	V _{OC} (Volt)	I _{SC} (mA/cm ²)	η (%)
0% Mn	41	0.51	8.18	1.71
0.5% Mn	45	0.53	7.19	1.74
1.5% Mn	51	0.53	8.41	2.27
3.5% Mn	51	0.53	9.03	2.44
8.5% Mn	50	0.56	7.37	2.06
15% Mn	36	0.50	4.34	0.78
25% Mn	—	—	—	—

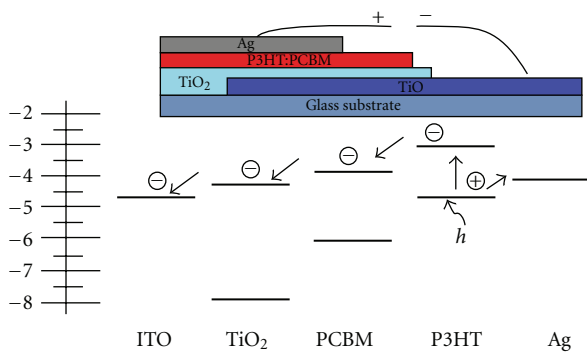
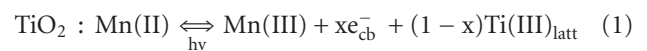


FIGURE 7: Schematic representation of the energy levels in our solar cell design (inset: the proposed solar cell assembly).

production of an electric dipole at the TiO₂/P3HT:PCBM interface or energy levels of Mn(II) ions are close to the valance band in the band gap of TiO₂ [38].

As the light illumination time is prolonged, this S shape disappears and the power conversion efficiency reaches 2.44% in 3.5% Mn²⁺-doped sample. Also dependency of the increase of the stabilization period on Mn amount reveals the

presence of a reaction between Ti and Mn atoms. Actually Saponjic and his coworkers propose the following reaction for this event [33]:



For this reason, the injection barrier of the TiO₂/P3HT:PCBM interface disappears and those electrons produced in active layer diffuse to TiO₂. However, there exists a decrease in conversion efficiency in the case of 8.5% Mn doping, although the light exposure duration is at the order of 20 minutes. Consistently, 15% Mn doping amount causes further decrease in the efficiency even after 30 minutes of the light exposure duration and solar cell parameters were lost in 25% Mn-doped sample.

In terms of dependence on the doping amount and light exposure, reasons of the S-shaped curve were tried to be clarified by inspirations from previous works done for both Mn and TiO₂ for other purposes. In regard to the evaluation of them in our case, the Mn(II) ions, embedded in the TiO₂ lattice, are excited by light resulting in that Mn(II) is converted to Mn(III). Then, the excited electrons are trapped producing in Ti(III). In this solar cell device, we can suppose that the electrons produced in active layer follow a path from

the TiO₂ to the ITO. As the light falls on the cell, the Mn (III) traps in the TiO₂ lattice occur for the electrons from the active layer. These electrons should pass to ITO side, but Mn (III) traps in the TiO₂ lattice capture them. The real reason of the observed S-shaped curve can be these Mn (III) traps. As long as the device is waited under the light illumination, electrons fill these trap levels. After the filling of the trap levels, the electrons transfer towards ITO effectively. In our opinion, the use of transition metal ions in hybrid solar cell is a serious candidate for the applications according to the results obtained experimentally.

4. Conclusion

The goal of this work is to exploit transition metal ions in hybrid organic solar cell. The Mn(II) ions were successfully adapted to TiO₂-based solar cells for the first time.

The S-like shape, which is observed occasionally, in the proposed solar cells, is attained in the scope of our hybrid design. The S-like shape is dependent on the Mn doping amounts and light exposure time (it disappears after long exposure time) for yielding an efficient solar cell. Maximum power conversion efficiency was obtained to be $\eta = 2.44\%$ for 3.5% Mn-doped TiO₂ solar cell. I_{sc} value is considered to be 9.03 mA/cm², which is a maximum in this efficient cell and Voc value is 0.53 V, which is a constant in all cells. This efficient cell reaches stability after 10-minute illumination. But further doping with Mn(II) ions resulted in decaying of the efficiency despite having longer stability periods. 25% Mn-doped cell could not reach desired stability and the cell parameters could not be measured for it even after 45-minute illumination.

References

- [1] A. P. Zoombelt, M. Fonrodona, M. M. Wienk, A. B. Sieval, J. C. Hummelen, and R. A. J. Janssen, "Photovoltaic performance of an ultrasmall band gap polymer," *Organic Letters*, vol. 11, no. 4, pp. 903–906, 2009.
- [2] C. J. Brabec, N. S. Sariciftci, and J. C. Hummelen, "Plastic solar cells," *Advanced Functional Materials*, vol. 11, no. 1, pp. 15–26, 2001.
- [3] S. Günes, H. Neugebauer, and N. S. Sariciftci, "Conjugated polymer-based organic solar cells," *Chemical Reviews*, vol. 107, no. 4, pp. 1324–1338, 2007.
- [4] H. Spanggaard and F. C. Krebs, "A brief history of the development of organic and polymeric photovoltaics," *Solar Energy Materials and Solar Cells*, vol. 83, no. 2-3, pp. 125–146, 2004.
- [5] J. Kalowekamo and E. Baker, "Estimating the manufacturing cost of purely organic solar cells," *Solar Energy*, vol. 83, no. 8, pp. 1224–1231, 2009.
- [6] N. S. Sariciftci, L. Smilowitz, A. J. Heeger, and F. Wudl, "Photoinduced electron transfer from a conducting polymer to buckminsterfullerene," *Science*, vol. 258, no. 5087, pp. 1474–1476, 1992.
- [7] M. M. Wienk, M. G. R. Turbiez, M. P. Struijk, M. Fonrodona, and R. A. J. Janssen, "Low-band gap poly(di-2-thienylthienopyrazine): fullerene solar cells," *Applied Physics Letters*, vol. 88, no. 15, Article ID 153511, 2006.
- [8] N. Camaioni, G. Ridolfi, G. Casalbore-Miceli, G. Possamai, and M. Maggini, "The effect of a mild thermal treatment on the performance of poly(3-alkylthiophene)/fullerene solar cells," *Advanced Materials*, vol. 14, no. 23, pp. 1735–1738, 2002.
- [9] J. K. J. van Duren, X. Yang, J. Loos et al., "Relating the morphology of poly(p-phenylene vinylene)/methanofullerene blends to solar-cell performance," *Advanced Functional Materials*, vol. 14, no. 5, pp. 425–434, 2004.
- [10] M. Reyes-Reyes, K. Kim, and D. L. Carroll, "High-efficiency photovoltaic devices based on annealed poly(3-hexylthiophene) and 1-(3-methoxycarbonyl)-propyl-1-phenyl-(6,6)C₆₁ blends," *Applied Physics Letters*, vol. 87, no. 8, Article ID 083506, 3 pages, 2005.
- [11] H. Yan, P. Lee, N. R. Armstrong et al., "High-performance hole-transport layers for polymer light-emitting diodes. Implementation of organosiloxane cross-linking chemistry in polymeric electroluminescent devices," *Journal of the American Chemical Society*, vol. 127, no. 9, pp. 3172–3183, 2005.
- [12] K. Kawano, R. Pacios, D. Poplavskyy, J. Nelson, D. D. C. Bradley, and J. R. Durrant, "Degradation of organic solar cells due to air exposure," *Solar Energy Materials and Solar Cells*, vol. 90, no. 20, pp. 3520–3530, 2006.
- [13] N. Koch, A. Vollmer, and A. Elschner, "Influence of water on the work function of conducting poly(3,4-ethylenedioxythiophene)/poly(styrenesulfonate)," *Applied Physics Letters*, vol. 90, no. 4, Article ID 043512, 2007.
- [14] M. P. de Jong, L. J. van Ijendoorn, and M. J. A. de Voigt, "Stability of the interface between indium-tin-oxide and poly(3,4-ethylenedioxythiophene)/poly(styrenesulfonate) in polymer light-emitting diodes," *Applied Physics Letters*, vol. 77, no. 14, pp. 2255–2257, 2000.
- [15] A. C. Arango, L. R. Johnson, V. N. Bliznyuk, Z. Schlesinger, S. A. Carter, and H. H. Hörhold, "Efficient titanium oxide/conjugated polymer photovoltaics for solar energy conversion," *Advanced Materials*, vol. 12, no. 22, pp. 1689–1692, 2000.
- [16] Y. Liu, M. A. Summers, C. Edder, J. M. J. Fréchet, and M. D. McGehee, "Using resonance energy transfer to improve exciton harvesting in organic-inorganic hybrid photovoltaic cells," *Advanced Materials*, vol. 17, no. 24, pp. 2960–2964, 2005.
- [17] J. Owen, M. S. Son, K. H. Yoo, B. D. Ahn, and S. Y. Lee, "Organic photovoltaic devices with Ga-doped ZnO electrode," *Applied Physics Letters*, vol. 90, no. 3, Article ID 033512, 2007.
- [18] C. Waldauf, M. Morana, P. Denk et al., "Highly efficient inverted organic photovoltaics using solution based titanium oxide as electron selective contact," *Applied Physics Letters*, vol. 89, no. 23, Article ID 233517, 2006.
- [19] S. K. Hau, H. L. Yip, N. S. Baek, J. Zou, K. O'Malley, and A. K. Y. Jen, "Air-stable inverted flexible polymer solar cells using zinc oxide nanoparticles as an electron selective layer," *Applied Physics Letters*, vol. 92, no. 25, Article ID 253301, 2008.
- [20] W. H. Baek, I. Seo, T. S. Yoon, H. H. Lee, C. M. Yun, and Y. S. Kim, "Hybrid inverted bulk heterojunction solar cells with nanoimprinted TiO₂ nanopores," *Solar Energy Materials and Solar Cells*, vol. 93, no. 9, pp. 1587–1591, 2009.
- [21] S. K. Hau, H. L. Yip, O. Acton, N. S. Baek, H. Ma, and A. K. Y. Jen, "Interfacial modification to improve inverted polymer solar cells," *Journal of Materials Chemistry*, vol. 18, no. 42, pp. 5113–5119, 2008.
- [22] Y. Hames, Z. Alpaslan, A. Kösemen, S. E. San, and Y. Yerli, "Electrochemically grown ZnO nanorods for hybrid solar cell applications," *Solar Energy*, vol. 84, no. 3, pp. 426–431, 2010.

- [23] Y. Kang, N. G. Park, and D. Kim, "Hybrid solar cells with vertically aligned CdTe nanorods and a conjugated polymer," *Applied Physics Letters*, vol. 86, no. 11, Article ID 113101, 2005.
- [24] S. Günes, K. P. Fritz, H. Neugebauer, N. S. Sariciftci, S. Kumar, and G. D. Scholes, "Hybrid solar cells using PbS nanoparticles," *Solar Energy Materials and Solar Cells*, vol. 91, no. 5, pp. 420–423, 2007.
- [25] Q. Qiao, Y. Xie, and J. T. McLeskey Jr., "Organic/inorganic polymer solar cells using a buffer layer from all-water-solution processing," *Journal of Physical Chemistry C*, vol. 112, no. 26, pp. 9912–9916, 2008.
- [26] L. Shena, X. D. Zhang, W. B. Guo, C. X. Liu, W. Dong, and S. P. Ruan, "Performance improvement of inverted polymer solar cells using V_2O_5 as an anode buffer layer," *Materials Science Forum*, vol. 663–665, pp. 865–868, 2011.
- [27] B. O'Regan and M. Grätzel, "A low-cost, high-efficiency solar cell based on dye-sensitized colloidal TiO_2 films," *Nature*, vol. 353, no. 6346, pp. 737–740, 1991.
- [28] K. Zhang, W. Xu, X. Li, S. Zheng, and G. Xu, "Effect of dopant concentration on photocatalytic activity of TiO_2 film doped by Mn non-uniformly," *Central European Journal of Chemistry*, vol. 4, no. 2, pp. 234–245, 2006.
- [29] J. P. Xu, Y. B. Lin, Z. H. Lu et al., "Enhanced ferromagnetism in Mn-doped TiO_2 films during the structural phase transition," *Solid State Communications*, vol. 140, no. 11–12, pp. 514–518, 2006.
- [30] W. Choi, A. Termin, and M. R. Hoffmann, "The role of metal ion dopants in quantum-sized TiO_2 : correlation between photoreactivity and charge carrier recombination dynamics," *Journal of Physical Chemistry*, vol. 98, no. 51, pp. 13669–13679, 1994.
- [31] Y. Wang, Y. Hao, H. Cheng et al., "Photoelectrochemistry of transition metal-ion-doped TiO_2 nanocrystalline electrodes and higher solar cell conversion efficiency based on Zn^{2+} -doped TiO_2 electrode," *Journal of Materials Science*, vol. 34, no. 12, pp. 2773–2779, 1999.
- [32] K. H. Ko, Y. C. Lee, and Y. J. Jung, "Enhanced efficiency of dye-sensitized TiO_2 solar cells (DSSC) by doping of metal ions," *Journal of Colloid and Interface Science*, vol. 283, no. 2, pp. 482–487, 2005.
- [33] Z. V. Saponjic, N. M. Dimitrijevic, O. G. Poluektov et al., "Charge separation and surface reconstruction: a Mn^{2+} doping study," *Journal of Physical Chemistry B*, vol. 110, no. 50, pp. 25441–25450, 2006.
- [34] W. Choi, A. Termin, and M. R. Hoffmann, "The role of metal ion dopants in quantum-sized TiO_2 : correlation between photoreactivity and charge carrier recombination dynamics," *Journal of Physical Chemistry*, vol. 98, no. 51, pp. 13669–13679, 1994.
- [35] J. Moser, M. Grätzel, and R. Gally, "Inhibition of electron-hole recombination in substitutionally doped colloidal semiconductor crystallites," *Helvetica Chimica Acta*, vol. 70, pp. 1596–1604, 1987.
- [36] A. Kumar, S. Sista, and Y. Yang, "Dipole induced anomalous S-shape I-V curves in polymer solar cells," *Journal of Applied Physics*, vol. 105, no. 9, Article ID 094512, 2009.
- [37] D. Gupta, M. Bag, and K. S. Narayan, "Correlating reduced fill factor in polymer solar cells to contact effects," *Applied Physics Letters*, vol. 92, no. 9, Article ID 093301, 2008.
- [38] T. Umeyayashi, T. Yamaki, H. Itoh, and K. Asai, "Analysis of electronic structures of 3d transition metal-doped TiO_2 based on band calculations," *Journal of Physics and Chemistry of Solids*, vol. 63, no. 10, pp. 1909–1920, 2002.



Hindawi

Submit your manuscripts at
<http://www.hindawi.com>

